ANDROLOGY

ISSN: 2047-2919

ANDROLOGY

ORIGINAL ARTICLE

Correspondence:
George L. Gerton, Center for Research on Reproduction and Women's Health, Department of Obstetrics and Gynecology, Perelman School of Medicine, University of Pennsylvania, 421 Curie Blvd., 1309 BRB II/III, Philadelphia, PA 19104-6160, USA. E-mail: gerton@mail.med.upenn.edu

Keywords:
epididymis, sperm function, spermatozoa

Received: 8-Aug-2013
Revised: 18-Sep-2013
Accepted: 20-Sep-2013

doi: 10.1111/j.2047-2927.2013.00147.x

Thiol changes during epididymal maturation: a link to flagellar angulation in mouse spermatozoa?

[1,2]T. W. Ijiri, [1]M. L. Vadnais, [1]A. P. Huang, [1]A. M. Lin, [3]L. R. Levin, [3]J. Buck and [1,4]G. L. Gerton

[1]Center for Research on Reproduction and Women's Health, Perelman School of Medicine, University of Pennsylvania, Philadelphia, PA, USA, [2]Department of Molecular Biosciences, Kyoto Sangyo University, Kyoto, Japan, [3]Department of Pharmacology, Weill Cornell Medical College, New York, NY, USA, and [4]Department of Obstetrics and Gynecology, Perelman School of Medicine, University of Pennsylvania, Philadelphia, PA, USA

SUMMARY

Caput epididymal wild-type spermatozoa and cauda epididymal spermatozoa from mice null for the adenylyl cyclase *Adcy10* gene are immotile unless stimulated by a membrane-permeant cyclic AMP analogue. Both types of spermatozoa exhibit flagellar angulation where the head folds back under these conditions. As sperm proteins undergo oxidation of sulfhydryl groups and the flagellum becomes more stable to external forces during epididymal transit, we hypothesized that ADCY10 is involved in a mechanism regulating flagellar stabilization. Although no differences were observed in global sulfhydryl status between caput and cauda epididymal spermatozoa from wild-type or *Adcy10*-null mice, two-dimensional fluorescence difference gel electrophoresis was performed to identify specific mouse sperm proteins containing sulfhydryl groups that became oxidized during epididymal maturation. A-kinase anchor protein 4, fatty acid-binding protein 9 (FABP9), glutathione S-transferase mu 5 and voltage-dependent anion channel 2 exhibited changes in thiol status between caput and cauda epididymal spermatozoa. The level and thiol status of each of these proteins were quantified in wild-type and *Adcy10*-null cauda epididymal spermatozoa. No differences in the abundance of any protein were observed; however, FABP9 in *Adcy10*-null cauda epididymal spermatozoa contained fewer disulfide bonds than wild-type sperm cells. In caput epididymal spermatozoa, FABP9 was detected in the cytoplasmic droplet, principal piece, midpiece, and non-acrosomal area of the head. However, in cauda epididymal spermatozoa, this protein localized to the perforatorium, post-acrosomal region and principal piece. Together, these results suggest that thiol changes during epididymal maturation have a role in the stabilization of the sperm flagellum.

INTRODUCTION

After spermatogenesis in the testis, spermatozoa pass sequentially through the caput and corpus epididymides and are retained in the cauda epididymis where they are stored until ejaculation (Cornwall, 2009). As spermatozoa migrate through the epididymis, they undergo intrinsic biochemical and functional modifications that result in the acquisition of motility and the ability to become capacitated for fertilization (Sullivan *et al.*, 2007). One of these alterations is an increase in the oxidation of sulfhydryl groups of sperm proteins resulting in more disulfide bonds and fewer free sulfhydryls. Earlier studies suggested that most sperm structures, such as the chromatin and tail components, gradually become stabilized by formation of disulfide bonds (Bedford & Calvin, 1974a,b; Calvin & Bedford, 1971). Similarly, labelling with the fluorescent thiol labelling agent monobromobimane (mBBr) demonstrates that the protein sulfhydryls of rat sperm structures become more oxidized to disulfide bonds during epididymal transit (Shalgi *et al.*, 1989).

The elevation of the ubiquitous second messenger cyclic AMP (cAMP) is an additional change that spermatozoa undergo as they move through the epididymis (White & Aitken, 1989). The in vitro addition of cell permeant cAMP analogues to hamster caput epididymal spermatozoa results in pre-maturely amplified motility and flagellar angulation where the sperm tails fold back on themselves. The addition of diamide, a sulfhydryl oxidant, prevents this phenomenon (Cornwall *et al.*, 1986, 1988). On the other hand, hamster cauda epididymal spermatozoa do not exhibit angularity when intracellular cAMP levels are raised (Cornwall *et al.*, 1988). However, these sperm cells will display flagellar angulation when dithiothreitol (DTT) is added (Cornwall & Chang, 1990). These observations have led to the concept that epididymal maturation results in stabilization of flagellar

structures through oxidation of protein sulfhydryls to disulfides thereby preventing against angulation when motility is stimulated by a rise in internal cAMP.

Two classes of adenylyl cyclases (ADCYs) convert ATP to cAMP: transmembrane ADCYs and 'soluble' ADCY10 (formerly SACY). ADCY10 activity was originally described over 35 years ago in the rat testis and, although present in somatic tissues, is most abundant and its activity most prevalent in the mammalian testis (Braun & Dods, 1975; Sinclair *et al.*, 2000). Most of cAMP in developing germ cells and mature sperm cells is generated by ADCY10, making this enzyme an essential component of cAMP signalling in spermatozoa (Hess *et al.*, 2005). Sperm cells from *Adcy10*-null males are immotile, owing to the lack of bicarbonate-induced ADCY10 activity, rendering them infertile (Esposito *et al.*, 2004). Their motility can be rescued by the addition of the membrane-permeant cAMP analogue, dibutyryl cAMP (dbcAMP); however, they are still unable to fertilize eggs (Hess *et al.*, 2005). Like caput epididymal spermatozoa of wild-type animals, *Adcy10*-null spermatozoa show flagellar angularity after the addition of dbcAMP and are not able to attach to the zona pellucida (Hess *et al.*, 2005). From these observations, we hypothesized that ADCY10 is required for flagellar stability and that flagellar angulation of *Adcy10*-null spermatozoa is caused by diminished disulfide bonding during epididymal maturation. A lack of ADCY10 may limit the ability of the sperm tail to become stabilized in the epididymis.

In this study, we used spermatozoa from *Adcy10*-null and wild-type mice for examination of flagellar angulation. We identified four sperm proteins: A-kinase anchor protein 4 (AKAP4), fatty acid-binding protein 9 (FABP9), glutathione S-transferase mu 5 (GSTM5) and voltage-dependent anion channel 2 (VDAC2) that exhibited changes in thiol status during epididymal maturation. Although these proteins were present at similar levels in spermatozoa from *Adcy10*-null and wild-type mice, on the basis of the experiments performed, FABP9 from *Adcy10*-null mouse spermatozoa contained fewer disulfide bonds.

MATERIALS AND METHODS

Purification of caput and cauda epididymal spermatozoa and protein extraction

All animal procedures were approved by the University of Pennsylvania Institutional Animal Care and Use Committee. Spermatozoa were collected from the caput and cauda epididymides of adult C57BL/6 (Charles River Laboratories, Wilmington, MA, USA) and *Adcy10*-null male mice of similar ages. The *Adcy10*-null genotype has been previously described (Hess *et al.*, 2005). Caput and cauda epididymal spermatozoa were extruded from the epididymides into phosphate-buffered saline (PBS: 2.68 mM KCl, 136.09 mM NaCl, 1.47 mM KH_2PO_4, 8.07 mM Na_2HPO_4, pH 7.4) containing protease inhibitors (Roche Applied Science, Indianapolis, IN, USA) and purified by centrifugation through a 35% (v/v) SupraSperm 100 solution (MidAtlantic Diagnostics, Mt. Laurel, NJ, USA) in PBS. Purified sperm cells were resuspended in PBS containing proteinase inhibitors at 4°C and counted in a haemocytometer.

For 2-D DIGE, sperm cells were concentrated by centrifugation at 10 000 ***g*** for 2 min then lysed by sonication at 4°C in cell lysis buffer (8 M urea, 40 mM Tris-HCl, pH 8.0, 4% (w/v) CHAPS) containing protease inhibitors. Approximately 1 μg of protein was collected from 4×10^4 spermatozoa. Protein lysates were used immediately.

For SDS-PAGE, sperm cells were concentrated by centrifugation at 10 000 ***g*** for 2 min, resuspended in PBS containing protease inhibitors, sonicated for 1 min, and then diluted in sample buffer [58 mM Tris-HCl, pH 6.8, 1.71% (w/v) SDS, 6% (v/v) glycerol, 0.0024% (w/v) bromophenol blue, with or without 100 mM DTT]. Samples were then vortexed, boiled for 5 min, and sonicated a second time. After centrifugation at 10 000 ***g*** for 5 min, the supernatants were recovered, snap-frozen and stored at −80°C until used.

Visualization of thiol groups with mBBr

For microscopic observation, 2.5×10^6 caput and cauda epididymal spermatozoa were collected as described above and distributed to four tubes (two caput and two cauda). The fluid volume in each tube was adjusted to 1 mL. DTT (154 μg) was added to epididymal sperm suspensions to a final concentration of 1 mM. All four samples were incubated for 10 min at 37°C. The samples were washed twice by centrifugation at 700 ***g*** for 5 min. The sperm pellet was resuspended in 500 μM mBBr (Life Technologies, Carlsbad, CA, USA) in PBS and incubated for 10 min in the dark at room temperature. After being washed with PBS, 200 μL of sperm suspension was spread on a glass slide and allowed to dry for 15 min. Slides were mounted with Fluoromount-G (Southern Biotechnology Associates, Birmingham, AL, USA) and covered with a coverslip. The samples were observed as described below.

For 1-D gel electrophoresis, 2×10^6 cauda epididymal spermatozoa were collected as described above and divided into two samples, but only one was treated with 5 mM DTT in PBS containing protease inhibitors. Samples were incubated for 10 min at 37°C. After being washed with PBS, 5 mM mBBr was added to the sperm cells for labelling at room temperature for 15 min in the dark. Spermatozoa were prepared for SDS-PAGE as described below. Samples were separated on a 12% (w/v) polyacrylamide gel and then protein fluorescence patterns were visualized by UV light (302 nm) using the Gel Doc 2000 Gel Documentation System (Bio-Rad Laboratories, Hercules, CA, USA). Gels were stained with Coomassie blue to determine protein loading. The values of protein fluorescence were compared with ImageJ software available online (http://rsb.info.nih.gov/ij/) (data not shown).

2-D fluorescence difference gel electrophoresis (2D-DIGE)

A CyDye DIGE Fluor saturation dye labelling protocol (GE Healthcare, Milwaukee, WI, USA) was used to label free cysteine thiols on whole sperm protein extracts. All labelling procedures for 2D-DIGE were carried out under nitrogen. Proteins were extracted as described above from four sperm populations: caput epididymal spermatozoa with or without disulfide reduction with Tris-(2-carboxyethyl) phosphine hydrochloride (TCEP) and cauda epididymal spermatozoa with or without disulfide reduction with TCEP. Each of the four sperm populations was analysed in triplicate. Each treatment (caput or cauda epididymal spermatozoa with or without TCEP) was done in triplicate on six mice (18 mice per treatment). The same 18 mice were used for the treatments with caput and cauda epididymal sperm proteins treated with or without TCEP.

To reduce disulfide bonds in sperm cells, 15 μg of each protein lysate were treated with 6 nmol TCEP for 1 h in the dark at 37°C before labelling with fluorescent dye. For both non-reduced and reduced samples, 5 μg of protein lysates from each sperm population were labelled with 4 nmol Cy5 for 30 min in the dark at 37°C. As an internal control, 10 μg of protein lysates from 12 sperm preparations (three samples from caput and cauda epididymal spermatozoa with or without reduction with TCEP) were pooled for a total of 120 μg of protein and labelled with 96 nmol Cy3 for 30 min in the dark at 37°C. Each protein lysate was mixed with equal volumes of DIGE sample buffer [7 M urea, 2 M thiourea, 4% (w/v) CHAPS, 2% (v/v) IPG buffer (non-linear pH 3-11), 130 mM DTT]. Unincorporated dye was removed by extracting the protein lysates with chloroform-methanol in the dark (Wessel & Flügge, 1984).

Five micrograms of Cy3-labelled internal control protein and Cy5-labelled protein from each experimental group were resuspended in 450 μL of rehydration buffer [7 M urea, 2 M thiourea, 4% (w/v) CHAPS, 0.5% (v/v) IPG buffer (non-linear pH 3–11), 130 mM DTT, 0.002% (w/v) bromophenol blue] and separated by 2-D gel electrophoresis. For the first dimension, samples in 450 μl of rehydration buffer were loaded in the IPGphor strip holder. The 24-cm Immobiline DryStrip (non-linear pH 3-11 gradient) (GE Healthcare) was placed in a holder and overlaid with ~5 mL of DryStrip cover fluid (GE Healthcare). Strips were hydrated under 50 V for 24 h and focused afterwards on the Ettan IPGphor II IEF system for a total of 80 kVh at 20°C. After electrophoresis, each strip was incubated with 7.5 mL equilibration buffer (6 M urea, 100 m M Tris-HCl, pH 8.0, 30% (v/v) glycerol, 2% (w/v) SDS, 0.5% (v/v) DTT, 0.002% (w/v) bromophenol blue) by rocking for 20 min. For the second dimension, the strips were placed on top of a 10–20% (w/v) gradient polyacrylamide gel containing SDS with low fluorescence glass plates (Jule Biotechnologies, Milford, CT, USA). SDS-PAGE was performed using the Ettan DALT*six* electrophoresis system.

Scanning and image analysis of 2D-DIGE

The Cy3 and Cy5 images were scanned in a Typhoon 9410 scanner (GE Healthcare) at a resolution of 100 μm (pixel size). DeCyder software v5.01 (GE Healthcare) was used to analyse the images. This software performs gel matching, quantification and statistical analyses. Spots were initially detected with the Differential In-Gel Analysis module of the software then protein-spot maps were matched from 12 gels with the Biological Variation Analysis module (Fig. 2). The gel-to-gel variations were normalized against the image of the Cy3-labelled internal control sample. A one-way analysis of variance (ANOVA) was used to compare changes in protein abundance and selected spots that underwent a mobility shift ($p < 0.05$). Identified spots were further screened using the Student's *t*-test to evaluate the low abundance spots in non-reduced cauda epididymal sperm protein samples. Spots were selected when they exhibited a 1.35-fold or more ($p < 0.071$) difference between non-reduced caput and cauda epididymal sperm proteins (Table S1).

In-gel digestion and mass spectrophotometry analysis of 2D-DIGE spots

To identify proteins that displayed differential patterns, individual spots were excised, in-gel digested, and analysed by mass spectrophotometry. For the preparative gel, a 500 μg aliquot of pooled protein from the four sperm populations was labelled with 400 nmol Cy3 and separated by 2-D gel electrophoresis as described above. The gel was scanned, placed in fixative (30% (v/v) methanol, 10% (v/v) acetic acid) for 3 days at room temperature, and stored in 5% v/v) acetic acid at 4°C until spot selection. Each spot position was determined and a pick list was created using DeCyder software. By the use of an Ettan spot picker (GE Healthcare), the designated gel sections were robotically excised, transferred to microplate wells and digested with trypsin (Strader *et al.*, 2006).

The digested proteins were identified by MALDI-TOF/TOF mass spectrometry in a 4700 Proteomics Analyzer mass spectrometer (Applied Biosystems, Foster City, CA, USA). MALDI plates were calibrated with six calibration spots, resulting in a mass accuracy of approximately ± 50 ppm. Peptide mass maps were acquired in reflectron mode (20-keV accelerating voltage) with 155-ns delayed extraction, averaging 2000 laser shots per spectrum. Trypsin autolytic peptides (*m/z* 842.51, 1045.56, and 2211.10) were used to calibrate each spectrum internally to a mass accuracy within 20 ppm. The MS/MS spectra were acquired with 4000 Series Explorer software v3.0 (Applied Biosystems).

The spectra were analysed using GPS Explorer software v3.5 (Applied Biosystems), which acts as an interface between the Oracle database containing raw spectra and a local copy of the MASCOT search engine v1.9.05. Peptide peaks with a signal/noise ratio greater than 5 and a mass between *m/z* 900 and 4000 were sought in the Swiss Institute of Bioinformatics SwissProt 53.0 database (269 293 sequences; 98 902 758 residues) with *Mus musculus* taxonomy (13 321 sequences). The 10 most intense peaks were automatically selected for MS/MS. Up to one missed trypsin cut was allowed, and the data were mined with oxidation of methionine and carbamidomethylation of cysteine as variable modifications.

For microsequencing, trypsin-digested samples were dissolved in 5 μL of 0.1% (v/v) formic acid and injected into a 10 cm long C18 capillary column with an autosampler (Eksigent Technologies, Dublin, CA, USA). The peptide samples were eluted by linearly increasing the mobile phase composition to 98% (v/v) solvent B [0.1% (v/v) formic acid in 100% acetonitrile] at a flow rate of 200 nL/min for 60 min by the use of a nanoLC system (Eksigent Technologies). Online nanospray (Thermo Fisher Scientific, Waltham, MA, USA) was used to spray the separated peptides into a LTQ mass spectrometer (Thermo Fisher Scientific). The raw data were acquired and analysed with Xcalibur 2.0 SR2 software (Thermo Fisher Scientific). The protein identification and database search were performed with MASCOT dll script of Xcalibur 2.0 SR2 using the combined MS and MS/MS data. A protein score of >70 with a protein confidence of identification >95% was considered acceptable. If a candidate protein was matched with two or more peptides, each peptide score of >30 was used as the threshold. For a low molecular weight protein ($M_r < 30\,000$), matching with a single peptide was also accepted if the peptide score was defined as >70.

Antibodies for immunoblot and indirect immunofluorescence analyses

The commercially available antibodies against AKAP4 and FABP9 did not recognize the proteins in our samples whereas

commercial anti-GSTM5 (14502-1-AP; Proteintech Group, Chicago, IL, USA) and anti-VDAC (PA1954a; Affinity Bioreagents, Golden, CO, USA) antibodies were successfully used for immunoblotting. Two rabbit polyclonal antibodies were produced for AKAP4 and FABP9. The antibody against AKAP4 was prepared in our laboratory, originally designated as anti-AKAP82, and was raised against the electrophoretically purified AKAP4 protein from the fibrous sheath of the sperm flagellum (Carrera *et al.*, 1994). Anti-perforatorium antibody (PERF15, i.e. FABP9) was a gift from Dr. Richard Oko (Oko *et al.*, 1990). The rabbit polyclonal antibody against the perforatorium was successfully used for immunoblotting, as described below, but did not show specific staining by indirect immunofluorescence. Instead, we used a newly created rabbit polyclonal antibody for mouse FABP9, which was a gift from Dr. Alex Travis, for indirect immunofluorescence (Selvaraj *et al.*, 2010). An antibody for α-tubulin (T5168; Sigma-Aldrich, Saint Louis, MO, USA) was used as an internal control for immunoblotting to compare protein abundance between wild-type and *Adcy10*-null mice. For immunoblot analysis, the following two secondary antibodies were used: alkaline phosphatase-conjugated, goat anti-mouse IgG + IgM whole antibody (GE Healthcare) and alkaline phosphatase-conjugated, goat anti-rabbit IgG whole antibody (GE Healthcare). For indirect immunofluorescence analysis, Alexa Fluor 488-conjugated goat anti-rabbit IgG (H + L) (Life Technologies) was used as a secondary antibody.

Immunoblot analysis and quantification

Wild-type and *Adcy10*-null cauda epididymal sperm protein extracts from 2×10^4 (α-tubulin), 1×10^5 (AKAP4), 5×10^5 (PERF15), 2×10^5 (GSTM5) and 1×10^6 (VDAC) sperm cells were boiled for 5 min then separated by SDS–polyacrylamide gel electrophoresis (PAGE) in polyacrylamide gels (10%: α-tubulin and AKAP4, 12%: GSTM5 and VDAC, 18%: PERF15) (Laemmli, 1970). The gels were then transferred to polyvinylidene difluoride membranes (Towbin *et al.*, 1979). After the membranes were blocked overnight with Tris-buffered saline-Tween [TBST: 125 mM NaCl, 25 mM Tris-HCl, pH 8.0, 0.1% (v/v) Tween 20] containing 5% (w/v) non-fat dry milk, they were washed in TBST and incubated for 1 h with the appropriate primary antibody (1 μg/mL mouse anti-α-tubulin antibody, 1 : 20 000 rabbit anti-AKAP4 antiserum, 1 : 3000 rabbit anti-PERF15 antiserum, 0.175 μg/mL rabbit anti-GSTM5 antibody, 1 μg/mL rabbit anti-VDAC antibody) in TBST containing 5% non-fat dry milk. After being washed with TBST, the blots were incubated for 1 h with the corresponding alkaline phosphatase-conjugated secondary antibody (1 : 5000) in TBST containing 5% non-fat dry milk, and after washing with TBST, the bound enzyme was developed with the Enhanced Chemifluorescence (ECF) Western Blotting Reagent Pack (GE Healthcare) according to the manufacturer's directions. ECF images were scanned in a Storm 860 scanner (GE Healthcare). The pixel volume of each band was quantified with ImageQuant software v5.2 (GE Healthcare) and the abundance of each protein was normalized against α-tubulin. The pixel volume results were analysed with *t*-tests and expressed as the mean ± standard deviation from experiments done in triplicate. A $p < 0.05$ was considered statistically significant. Negative controls using normal sera for AKAP4 and PERF15, purified IgG, or secondary antibody alone were used to check for specificity.

Detection of disulfide cross-linking of sperm proteins

Cauda epididymal spermatozoa from wild-type and *Adcy10*-null mice were collected as described above. For DTT-treated samples, 100 mM DTT was added, and samples were incubated at room temperature for 10 min. Samples not treated with DTT were incubated at room temperature for 10 min. After the addition of 5 mM iodoacetic acid to DTT-treated and untreated samples, the pH was adjusted to 7.2. Samples were incubated for 30 min in the dark at room temperature. Samples were sonicated then centrifuged at 10 000 ***g*** for 5 min, and the supernatants were snap-frozen and stored at −80°C.

SDS-PAGE, immunoblotting, scanning and data quantification were performed as described above with the following modifications: 1.5×10^5 (AKAP4), 7.5×10^5 (PERF15), 3×10^5 (GSTM5) and 1.5×10^6 (VDAC) cauda epididymal spermatozoa were used. The dilutions and concentrations of the primary antibodies were as follows: 1 : 15000 anti-AKAP4, 1 : 2250 anti-PERF15, 0.233 μg/mL anti-GSTM5 and 1.33 μg/mL anti-VDAC).

Indirect immunofluorescence analysis

One million caput or cauda epididymal spermatozoa, collected as described above, were attached to polylysine-coated coverslips for 15 min then fixed and permeabilized with acetone/methanol (1 : 1) for 1 min at −20°C. After extensive washing with PBS, the coverslips were incubated overnight at 4°C with 10% goat serum in PBS (blocking solution). The following day, coverslips were rinsed with PBS and incubated for 1 h at 37°C with anti-FABP9 antibody (1 : 100) diluted in blocking solution. After being washed with PBS, the coverslips were incubated for 1 h at 37°C with Alexa Fluor 488-conjugated goat anti-rabbit IgG (1 : 500) diluted in blocking solution. The coverslips were washed with PBS, mounted on slides with 15 μL of Fluoromount-G, observed with a Nikon Eclipse TE 2000-U inverted microscope (Nikon Instruments, Melville, NY, USA), and photographed with a CFW-1310C digital FireWire camera (Scion, Frederick, MD, USA) with NIH ImageJ. Nomarski differential interference contrast micrographs were photographed in parallel with the fluorescence images. Negative controls with normal sera or secondary antibody alone were also used to check for specificity.

RESULTS

A global difference in protein thiol status was not observed between wild-type and Adcy10-null spermatozoa

The fluorescent stain mBBr was used to visualize free sulfhydryl groups in whole caput and cauda epididymal spermatozoa from wild-type and *Adcy10*-null mice. Spermatozoa treated with DTT to reduce disulfide bonds were used as controls. Intense staining was detected throughout the entire sperm cells in control samples (DTT treated). Similar to the controls, caput epididymal spermatozoa displayed fluorescent staining in the heads and flagella (Fig. 1A). However, cauda epididymal spermatozoa had only faint fluorescent signals throughout the cells (Fig. 1B). There were no obvious differences between wild-type and *Adcy10*-null spermatozoa in these comparisons. Next, we investigated the band patterns of wild-type and *Adcy10*-null cauda epididymal sperm proteins labelled with mBBr. DTT-treated spermatozoa were used as controls. No difference between the

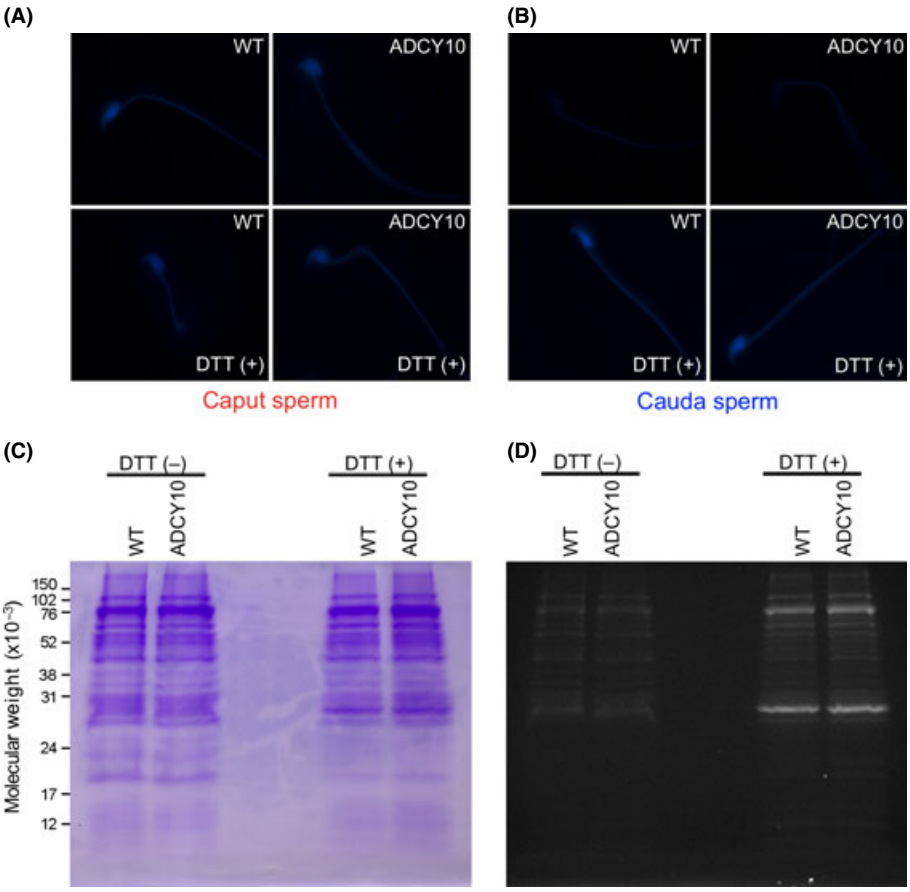

Figure 1 Characterization of thiol status between wild-type and *Adcy10*-null caput and cauda epididymal spermatozoa by the use of monobromobimane (mBBr) fluorescence. mBBr staining for proteins from caput (A) and cauda (B) epididymal spermatozoa from wild-type and *Adcy10*-null mice, which were non-reduced (top) or reduced with DTT (bottom). 1-D gel electrophoresis of mBBr-labelled non-reduced (DTT−) and reduced (DTT+) cauda epididymal sperm proteins from wild-type or *Adcy10*-null mice, stained by Coomassie blue (C) and protein fluorescence patterns visualized by UV light (D). Although a difference in thiol status was observed between caput and cauda epididymal spermatozoa, no difference was seen between wild-type and *Adcy10*-null sperm cells.

fluorescence patterns of wild-type and *Adcy10*-null cauda epididymal spermatozoa were observed (Fig. 1D).

AKAP4, FABP9, GSTM5 and VDAC2 exhibit changes in thiol status during epididymal maturation

We did not detect a change in global disulfide bonding between wild-type and *Adcy10*-null cauda epididymal sperm proteins, which prompted us to examine more closely the disulfide bond status of individual proteins by proteomic techniques. We used 2-D DIGE to identify proteins in which sulfhydryl groups became oxidized during epididymal maturation. Differences in disulfide bonding were detected by comparing samples from caput and cauda epididymal spermatozoa whose proteins were reduced or not reduced with TCEP before labelling with the fluorescent dye Cy5. As the internal control, Cy3-labelled proteins demonstrated a highly reproducible pattern of fluorescent protein spots in many scanned images (data not shown).

We identified multiple spots as sperm proteins that changed their thiol status during epididymal maturation. Initially, approximately 3000 spots in each gel were identified with more than 1500 of them being present in all 12 gels. Protein abundance changes of 755 spots between the four protein populations were shown to be statistically significant ($p < 0.05$) by one-way ANOVA. From these, 57 spots were selected as low abundant spots, only in non-reduced cauda epididymal sperm populations, from their graph view with DeCyder software (an outline of this procedure is shown in Fig. 2). Furthermore, using the Student's *t*-test, we determined that 23 protein spots exhibited differential abundance of 1.35-fold or more ($p < 0.05$) between non-reduced caput and cauda epididymal sperm populations (Table S1). Twenty-three candidate spots for thiol status change were selected from analytical gels; however, three of them were missing from the preparative gel (Fig. 2). Finally, 20 spots were picked from the preparative gel for mass spectrometric analysis. The positions of these spots are shown on analytical gels (Fig. 3).

The sequence information for 18 spots was obtained, and the peptide matches to entries in the database are shown in Table S1. Some spots contained peptides that corresponded to more than one protein. GSTM5 and VDAC2 were identified from single spots (#2281 and #1909 respectively). However, AKAP4 was identified from three spots (#2281, #2781 and #2796). All three spots possessed different isoelectric points. Spot #2281 was of higher molecular weight (M_r 26 617) than the other two spots (#2781 and #2796: M_r 15 079) and corresponded by size and peptide sequences to the 'Pro' domain of the AKAP4 precursor (Johnson *et al.*, 1997). The peptide from spots #2781 and #2796 aligned 34 amino acids downstream from the pro-AKAP4 cleavage site.

Twelve spots (#2652, #2663, #2672, #2725, #2781, #2796, #2803, #2815, #2816, #2864, #2883 and #2966) were derived from FABP9. These spots showed similar molecular weights (M_r ~15,079) yet could be classified into two major clusters. The first cluster (#2652, #2663, #2672, and #2725) was positioned slightly higher than the second cluster (#2781, #2796, #2803, #2815, #2864 and #2883) on the 2-D gel (Fig. 3). #2816 was detected between the first and second clusters whereas #2966 was detected lower than the second cluster. It is important to note that the isoelectric points of FABP9 ranged widely on the 2-D gel. The 12 spots could be divided into seven types that range from acidic to basic:

Figure 2 A summary of the screening procedure for protein spots that change their thiol status during epididymal maturation. Over 3000 spots were identified with more than 1500 being represented in all gels. After statistical analysis and comparison between non-reduced caput and cauda epididymal spermatozoa, 23 spots were chosen for characterization. Only 20 of those spots were present on the preparative gel. The graph in the top right indicates protein abundance in reduced caput (Cp+), non-reduced caput (Cp−), reduced cauda (Cd+) and non-reduced cauda (Cd−) epididymal spermatozoa.

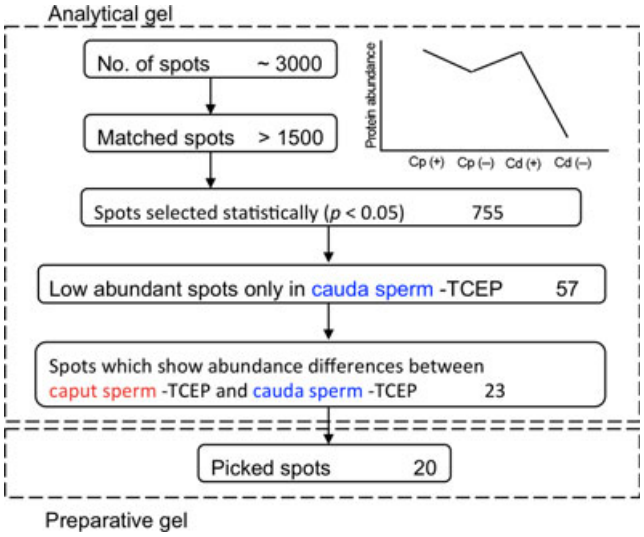

#2781, two spots (#2652 and #2796), two spots (#2663 and #2803), two spots (#2672 and #2815), three spots (#2725, #2816 and #2864), #2966 and #2883. These results demonstrated that FABP9 underwent a variety of post-translational modifications. Using NetPhos 2.0 (http://www.cbs.dtu.dk/services/NetPhos/), we predicted that four serine, three threonine and two tyrosine residues were available as potential phosphorylation sites in FABP9 (data not shown).

Six spots (#2008, #2602, #2652, #2749, #2781 and #2966) were identified as keratin 1 (KRT1), keratin 4 (KRT4), keratin 10 (KRT10) or keratin 15 (KRT15). In addition, the α- and β1-subunits of haemoglobin was detected in spot #3089. We did not pursue analysis of these proteins because there are limited data concerning their expression during spermatogenesis and their presence in mature spermatozoa.

AKAP4, FABP9, GSTM5 and VDAC2 are present at similar levels in wild-type and Adcy10-null spermatozoa

SDS-PAGE and immunoblotting were used to determine the relative levels of AKAP4, FABP9, GSTM5 and VDAC2 in wild-type and *Adcy10*-null cauda epididymal spermatozoa. ImageQuant software was used to measure the pixel volume of each protein band, which was then used to quantify and compare the relative abundance of AKAP4, FABP9, GSTM5 and VDAC2. To normalize data, α-tubulin was used as an internal control. Normalized volumes were expressed as the wild-type/*Adcy10*-null ratio. The pixel volumes of AKAP4, FABP9, GSTM5 and VDAC2 were not significantly different between wild-type and *Adcy10*-null sperm cells (Fig. 4). Three independent wild-type and *Adcy10*-null epididymal sperm populations were examined, and similar results were obtained in each case.

Compared with those from wild-type mice, Adcy10-null cauda epididymal spermatozoa have few disulfide bonds in FABP9

The presence of disulfide bonds in AKAP4, FABP9, GSTM5 and VDAC2 was evaluated by SDS-PAGE and immunoblotting with non-reduced cauda epididymal sperm proteins from wild-type and *Adcy10*-null mice. All four proteins in non-reduced sperm samples (arrow heads) were identified at the top of the gel, suggesting that these proteins were present in large disulfide-bonded complexes (Fig. 5). In non-reduced samples, antibodies against FABP9, GSTM5 and VDAC proteins detected faint bands at the expected sizes of M_r 15 000, 26 000 and 31 000

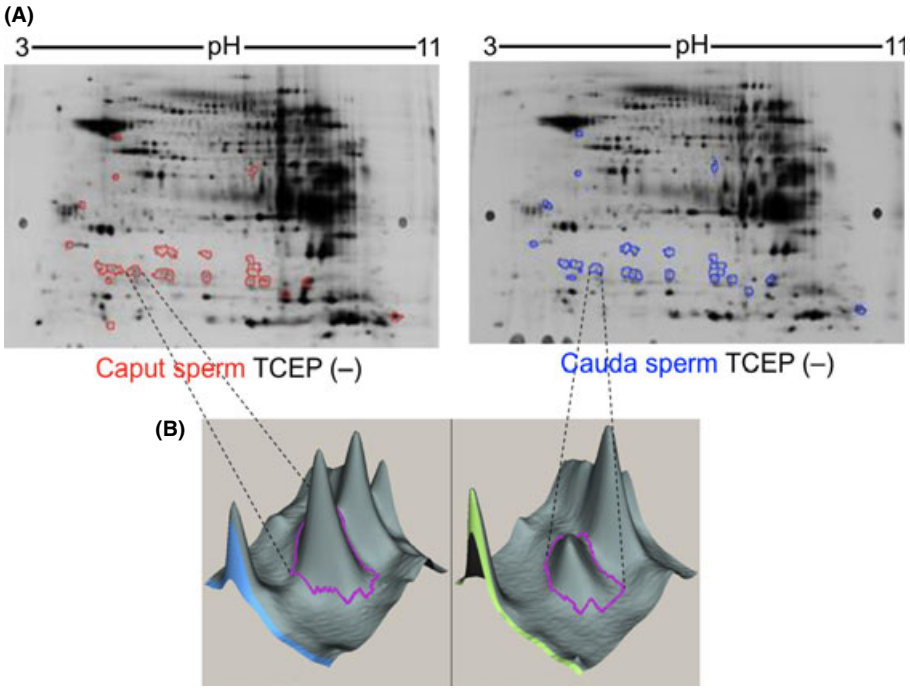

Figure 3 Scanned 2-D gel image highlighting the position of the identified spots as well as a 3-D view of a representative spot. (A) Gel images of Cy5-labelled protein samples in caput and cauda epididymal spermatozoa without TCEP. Coloured circles indicate the differentially labelled 23 spots. (B) 3-D rendering of fluorescence intensity values for a single spot.

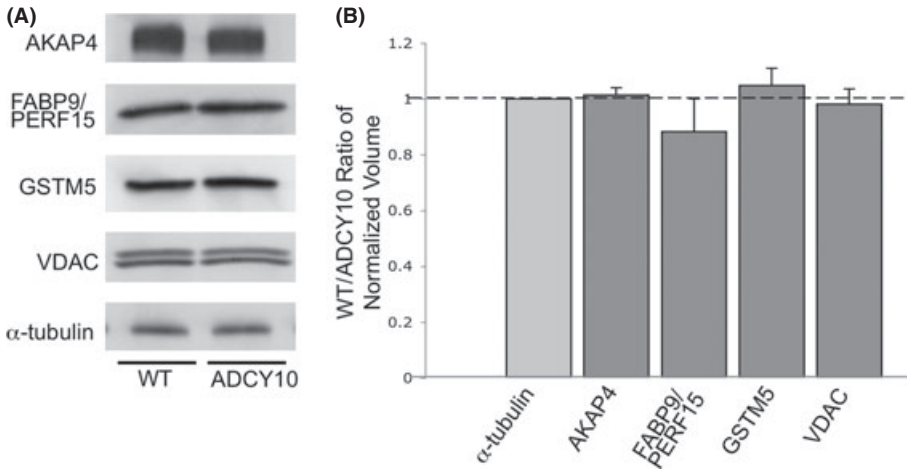

Figure 4 Protein abundance of AKAP4, FABP9, GSTM5 and VDAC2 in wild-type and *Adcy10*-null cauda epididymal spermatozoa. (A) Immunoblot analysis of the four identified sperm proteins and α-tubulin in wild-type (left) and *Adcy10*-null (right) cauda epididymal spermatozoa. (B) The pixel volumes of the protein bands were normalized against that of α-tubulin. AKAP4, FABP9, GSTM5 and VDAC2 were not found to be in lower amounts in *Adcy10*-null spermatozoa.

respectively. No bands were observed at M_r 82 000 in non-reduced samples when the AKAP4 antibody was used. The monomeric form of FABP9 was detected at greater levels in the non-reduced *Adcy10*-null sperm protein extracts than in proteins from non-reduced wild-type spermatozoa indicating that a subset of FABP9 proteins were not cross-linked into high molecular weight complexes in *Adcy10*-null spermatozoa as was found for wild-type sperm cells.

FABP9 localizes in the cytoplasmic droplet of wild-type caput epididymal spermatozoa

Indirect immunofluorescence was used to detect FABP9 in caput and cauda epididymal spermatozoa from wild-type mice. In caput epididymal spermatozoa, FABP9 was detected intensely in the cytoplasmic droplet as well as along the principal piece, midpiece and the non-acrosomal area of the head (Fig. 6). However, this protein localized to the perforatorium, post-acrosomal region and principal piece of cauda epididymal spermatozoa. No signal was observed when normal sera were used (data not shown).

DISCUSSION

The pivotal role of disulfide bonds for sperm structure and flagellar straightness has been recognized for over 40 years. A decrease in the fluorescent thiol labelling agent mBBr during epididymal maturation has also been reported in rat (Shalgi *et al.*, 1989) and mouse (Conrad *et al.*, 2005), indicating the oxidation of thiols to disulfides. Hamster sperm proteins of 85–94, 50–55 and 35–40 kDa, which are rich in sulfhydryl groups, are involved in the maintenance of flagellar straightness (Cornwall & Chang, 1990). However, the identity of these proteins has never been analysed. This study is the first comprehensive identification of sperm proteins that change their thiol status during transit through the epididymis.

There are four major hypotheses for the cause of flagellar angulation in spermatozoa: osmolality disturbances (Yeung

Figure 5 Demonstration of AKAP4, FABP9, GSTM5 and VDAC2 thiol status during epididymal maturation and comparison of disulfide cross-linking of these proteins in wild-type and *Adcy10*-null cauda epididymal spermatozoa. Immunoblot analysis of AKAP4, FABP9, GSTM5 and VDAC2 from reduced (DTT+) and non-reduced (DTT−) wild-type and *Adcy10*-null cauda epididymal spermatozoa. All four proteins were trapped on the bottom of the sample well in non-reduced sperm proteins (arrow-heads). FABP9 was detected at greater levels in the non-reduced *Adcy10*-null sperm protein extracts than in proteins from non-reduced wild-type spermatozoa indicating that *Adcy10*-null cauda epididymal sperm proteins contained fewer disulfide bonds than wild-type sperm cells. Antibodies against AKAP4, FABP9, GSTM5 and VDAC proteins detected bands of the predicted sizes of M_r 82 000, 15 000, 26 000 and 31 000 respectively.

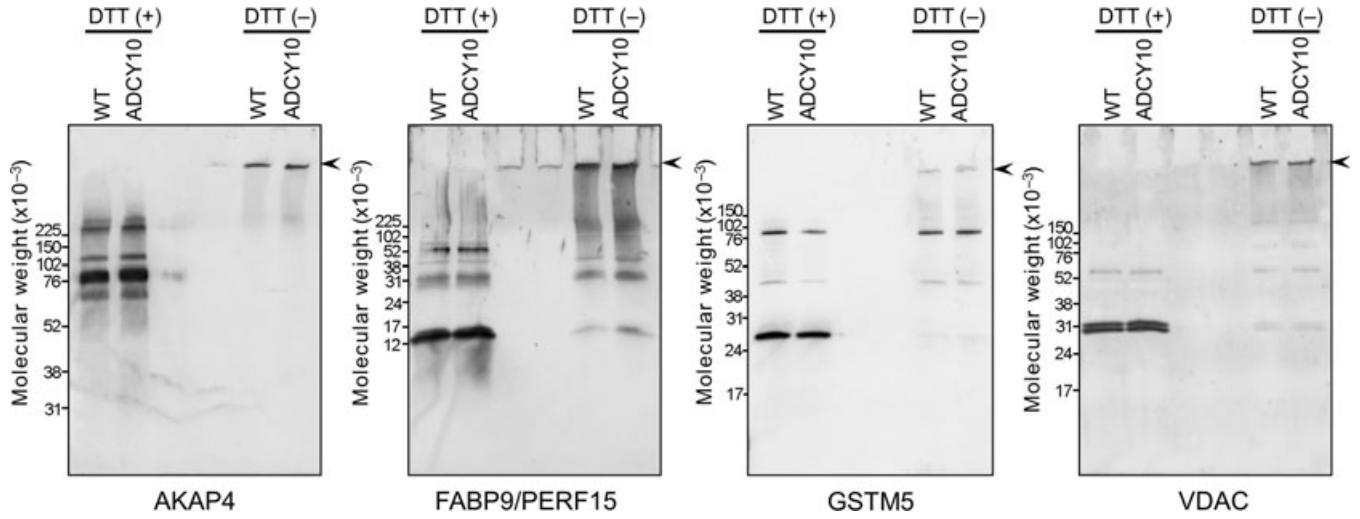

et al., 1999), selenium deficiencies (Schneider *et al.*, 2009), gene mutations in male germ cells (Cheng *et al.*, 2007) and abnormal annulus formation (Ihara *et al.*, 2005). The thiol peroxidase, glutathione peroxidase 4 (GPx4) and the disulfide isomerase/reductase, thioredoxin-glutathione reductase (TGR), have been proposed to play a key role in preventing flagellar angulation through formation of disulfide bonds. Mitochondrial GPx4 disruption in mice results in flagellar angulation and increases the extent of free sulfhydryl groups on epididymal sperm proteins (Schneider *et al.*, 2009). The abundance and status of GPx4 and TGR proteins should be investigated between wild-type and ADCY10-null spermatozoa. Sperm cells from *Adcy10*-null males are immotile and demonstrate flagellar angularity after the addition of dbcAMP (Hess *et al.*, 2005). We report similar findings with ADCY10-null spermatozoa. Here, we provide evidence that flagellar angulation in ADCY10-deficient spermatozoa is associated with diminished disulfide bond formation involving the FABP9 protein. We speculate that these thiol status changes may result from gene mutations or osmolality disturbances. FABP9 and GSTM5 are downstream targets of TGR in the rat testis (Su *et al.*, 2005).

In the last decade, the combination of 2-D electrophoresis and mass spectrometric techniques has made it possible to identify sperm proteins contained in specific compartments of the sperm cell (Cao *et al.*, 2006). Recently, the more sophisticated 2-D DIGE method has made it feasible to detect minute differences in abundance of protein populations, leading to the identification of sperm proteins that have roles in epididymal maturation and capacitation (Baker *et al.*, 2005, 2006; Ijiri *et al.*, 2011). DIGE Fluor saturation dyes are optimized for the labelling of cysteine residues on reduced proteins. However, in these experiments, we applied this dye for detection of non-reduced as well as reduced caput and cauda epididymal sperm proteins (Fig. 2).

Using this technique, we identified four sperm proteins (Table 1: AKAP4, FABP9, GSTM5 and VDAC2) that displayed differences in disulfide bonds between caput and cauda epididymal sperm cells (Fig. 3). GSTM5 and VDAC2 were identified from single spots. Of the four proteins identified, AKAP4 (M_r 82 000) was the only protein identified that corresponded to the size of proteins predicted to be involved in flagellar straightness of hamster spermatozoa (Cornwall & Chang, 1990). FABP9 was recovered from 12 spots that had similar molecular weights (M_r 15 000) with a range of various isoelectric points. Because FABP9 was detected in many spots from whole sperm lysate on 2-D gel, it may be possible to detect more candidate proteins using a protein population from the sperm tail alone, excluding FABP9 associated with the sperm head. Fractionation of sperm proteins to eliminate lower molecular weight proteins (<15 kDa) may also yield other candidate proteins that undergo oxidation of sulfhydryl groups during transit from the caput to the cauda epididymis.

Two of the proteins we identified in this study, AKAP4 and VDAC2, were not previously known to undergo further sulfhydryl oxidation during the course of epididymal maturation. AKAP4 is specific to male germ cells and tethers cAMP-dependent protein kinase to the fibrous sheath of the flagellum (Carrera *et al.*, 1994; Fulcher *et al.*, 1995a; Visconti *et al.*, 1997). Immunoelectron microscopy indicates that mouse AKAP4 is present in the longitudinal columns and transverse ribs of the sperm fibrous sheath (Johnson *et al.*, 1997). *Akap4*-null male mice are infertile; their spermatozoa do not display progressive motility because they do

Figure 6 Indirect immunofluorescence of wild-type caput and cauda epididymal spermatozoa probed with the anti-FABP9 antibody. This protein was detected intensely in the cytoplasmic droplet as well as along the principal piece, midpiece and the non-acrosomal area of the head in caput epididymal spermatozoa (top). FABP9 localized to the perforatorium, post-acrosomal region and principal piece in cauda epididymal spermatozoa (bottom). The corresponding Nomarski differential interference contrast micrographs are to the right of each fluorescence image.

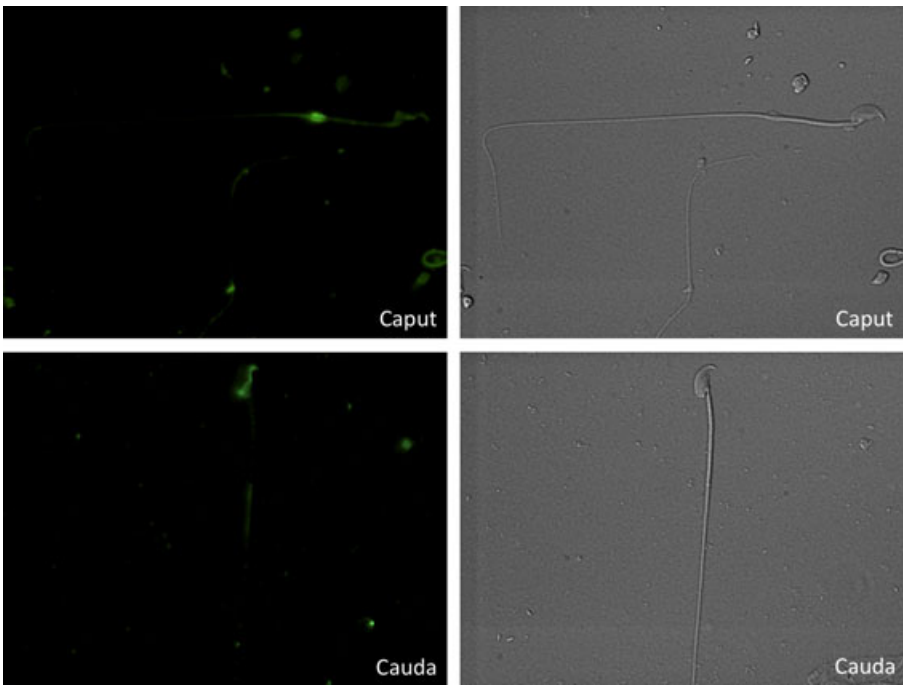

Table 1 Summary of the four proteins (AKAP4, FABP9, GSTM5 and VDAC2) identified in this analysis. AKAP4 is located in the fibrous sheath and is involved in signal transduction. FABP9 is located in the perforatorium of cauda epididymal sperm cells and is involved in structural integrity. GSTM5 is involved in oxidative defence and is located in the fibrous sheath. VDAC2 is found in the midpiece and acrosome and is responsible for ion regulation

Protein	Function	Location in spermatozoa
AKAP4	Structural and cytoskeletal Signal transduction	Fibrous sheath
FABP9/ PERF15	Structural and cytoskeletal	Perforatorium
GSTM5	Oxidative defence	Fibrous sheath
VDAC2	Structural and cytoskeletal Ion channel	Midpiece and acrosome

AKAP4, A-kinase anchor protein 4; FABP9, fatty acid-binding protein 9; GSTM5, glutathione S-transferase mu 5; VDAC2, voltage-dependent anion channel 2.

not form a functional fibrous sheath (Miki *et al.*, 2002). In this study, we identified the proAKAP4 polypeptide that corresponds to the 'PRO' domain of the precursor. In previous studies, this 179 amino acid fragment ran with a molecular weight of approximately 26 000, which is similar to our finding here. However, the actual molecular weight is calculated to be 19 994. In our previous work, we rationalized the ~6000 molecular weight estimation to result from anomalous electrophoretic behaviour. However, the finding of GSTM5 peptides in the same spot raises the possibility that the 'PRO' domain of proAKAP4 and a fragment of GSTM5 are linked; we think this unlikely as the molecular weight of GSTM5 itself is 26 634 (Fulcher *et al.*, 1995b). VDACs are small pore-forming proteins first identified in outer mitochondrial membranes and play various biological roles in somatic cells (Colombini, 1979). VDAC2 locates to the acrosomal region as well as outer dense fibres of the bovine sperm flagellum (Hinsch *et al.*, 2004; Triphan *et al.*, 2008).

GSTM5 and FABP9 are potential targets for thiol oxidation in spermatozoa. GSTM5 is a germ cell-specific member of the μ-class GST family and serves to protect sperm from oxidative stress. Immunoblot analysis with an antibody to μ-class GSTs indicated this protein in isolated fibrous sheaths from mouse cauda epididymal spermatozoa (Fulcher *et al.*, 1995b). Furthermore, hexokinase type 1 is tethered in the principal piece region by the sperm-specific variant of muscle-type phosphofructokinase, which in turn is bound tightly to GSTM5 in the fibrous sheath, demonstrating the compartmentalization of specific glycolytic enzymes in the sperm cell (Nakamura *et al.*, 2010). FABP9 was originally identified as the major protein of the rat perforatorium between the inner acrosomal membrane and the outer face of the nuclear envelope in the sperm head (Oko & Morales, 1994) and later recognized in the perforatorium of mouse spermatozoa (Korley *et al.*, 1997). In rat spermatogenic cells from mid-pachytene spermatocytes to step 19 spermatids, anti-perforatorium antibodies react to the cytoplasm and nuclei of the sperm head (Oko & Clermont, 1991). We demonstrated that FABP9 was located in the perforatorium and post-acrosomal region in cauda epididymal spermatozoa (Fig. 6). These findings are similar to what has been previously reported (Selvaraj *et al.*, 2010). Interestingly, we detected FABP9 in the midpiece and cytoplasmic droplet of caput epididymal spermatozoa (Fig. 6). Proteomic analysis suggests that the mitochondrial capsule of rat spermatozoa contains minor amounts of FABP9 (Maiorino *et al.*, 2005). The amount of FABP9 in the mitochondria of cauda epididymal mouse spermatozoa may be too low to be detected by indirect immunofluorescence or the epitopes recognized by the antibody may be cryptic under those conditions.

The four proteins identified in this study were all present at similar amounts in wild-type and *Adcy10*-null sperm cells (Fig. 4). On the basis of the experiments performed here, we demonstrated that only FABP9 contained fewer disulfide bonds in *Adcy10*-null cauda epididymal spermatozoa than in wild-type sperm cells (Fig. 5). However, AKAP4, GSTM5 and VDAC2 should not be eliminated as candidate proteins displaying thiol status changes. The proportion of disulfide bonds in reduced cauda epididymal spermatozoa may simply be less significant in these proteins, owing to the large number of bonds already present. The overall status of thiols and disulfides was similar between wild-type and *Adcy10*-null spermatozoa, but a diminution of free sulfhydryl groups was observed between caput and cauda epididymal spermatozoa, regardless of the genotype (Fig. 1). These data suggest the aberration of disulfide bonding in sperm proteins that may affect flagellar morphology between wild-type and *Adcy10*-null spermatozoa is not global and may be restricted to a limited number of proteins.

Male infertility has various causes, and the majority of cases remain idiopathic. Flagellar angulation has been suggested as one of the causes of male infertility. An example of this is the *c-ros* knockout and GPX5-Tag2 transgenic mouse models that are infertile owing to flagellar angulation (Cooper *et al.*, 2004). Our results may contribute to the diagnosis and treatment of male infertility caused by sperm flagellar angulation due to diminished disulfide bonds. These results suggest that oxidization of sulfhydryl groups during maturation covers a wide area of the spermatozoa and that most of the proteins that contain disulfide bonds are structural or cytoskeletal proteins.

ACKNOWLEDGEMENTS

This work was supported by NIH grants: R01HD051999, R01HD057144, T32HD007305 and P30ES013508, R01HD059913. We thank members of the Gerton laboratory for their encouragement and support with this project. We are also grateful to Drs. Richard Oko and Alex Travis for gifts of antibodies to FABP9.

CONFLICT OF INTEREST

The authors declare that there is no conflict of interest that could be perceived as prejudicing the impartiality of the research reported.

REFERENCES

Baker MA, Witherdin R, Hetherington L, Cunningham-Smith K & Aitken RJ. (2005) Identification of post-translational modifications that occur during sperm maturation using difference in two-dimensional gel electrophoresis. *Proteomics* 5, 1003–1012.

Baker MA, Hetherington L & Aitken RJ. (2006) Identification of SRC as a key PKA-stimulated tyrosine kinase involved in the capacitation-associated hyperactivation of murine spermatozoa. *J Cell Sci* 119, 3182–3192.

Bedford JM & Calvin HI. (1974a) Changes in -S-S- linked structures of the sperm tail during epididymal maturation, with comparative observations in sub-mammalian species. *J Exp Zool* 187, 181–204.

Bedford JM & Calvin HI. (1974b) The occurrence and possible functional significance of -S-S- crosslinks in sperm heads, with particular reference to eutherian mammals. *J Exp Zool* 188, 137–155.

Braun T & Dods RF. (1975) Development of a Mn-2+-sensitive, "soluble" adenylate cyclase in rat testis. *Proc Natl Acad Sci USA* 72, 1097–1101.
Calvin HI & Bedford JM. (1971) Formation of disulphide bonds in the nucleus and accessory structures of mammalian spermatozoa during maturation in the epididymis. *J Reprod Fertil Suppl* 13, 65–75.
Cao W, Gerton GL & Moss SB. (2006) Proteomic profiling of accessory structures from the mouse sperm flagellum. *Mol Cell Proteomics* 5, 801–810.
Carrera A, Gerton GL & Moss SB. (1994) The major fibrous sheath polypeptide of mouse sperm: structural and functional similarities to the A-kinase anchoring proteins. *Dev Biol* 165, 272–284.
Cheng Y, Buffone MG, Kouadio M, Goodheart M, Page DC, Gerton GL *et al.* (2007) Abnormal sperm in mice lacking the Taf7l gene. *Mol Cell Biol* 27, 2582–2589.
Colombini M. (1979) A candidate for the permeability pathway of the outer mitochondrial membrane. *Nature* 279, 643–645.
Conrad M, Moreno SG, Sinowatz F, Ursini F, Kölle S, Roveri A *et al.* (2005) The nuclear form of phospholipid hydroperoxide glutathione peroxidase is a protein thiol peroxidase contributing to sperm chromatin stability. *Mol Cell Biol* 25, 7637–7644.
Cooper TG, Yeung C-H, Wagenfeld A, Nieschlag E, Poutanen M, Huhtaniemi I *et al.* (2004) Mouse models of infertility due to swollen spermatozoa. *Mol Cell Endocrinol* 216, 55–63.
Cornwall GA. (2009) New insights into epididymal biology and function. *Hum Reprod Update* 15, 213–227.
Cornwall GA & Chang TS. (1990) Characterization of sulfhydryl proteins involved in the maintenance of flagellar straightness in hamster spermatozoa. *J Androl* 11, 168–181.
Cornwall GA, Smyth TB, Vindivich D, Harter C, Robinson J & Chang TS. (1986) Induction and enhancement of progressive motility in hamster caput epididymal spermatozoa. *Biol Reprod* 35, 1065–1074.
Cornwall GA, Vindivich D, Tillman S & Chang TS. (1988) The effect of sulfhydryl oxidation on the morphology of immature hamster epididymal spermatozoa induced to acquire motility in vitro. *Biol Reprod* 39, 141–155.
Esposito G, Jaiswal BS, Xie F, Krajnc-Franken MAM, Robben TJAA, Strik AM *et al.* (2004) Mice deficient for soluble adenylyl cyclase are infertile because of a severe sperm-motility defect. *Proc Natl Acad Sci USA* 101, 2993–2998.
Fulcher KD, Mori C, Welch JE, O'Brien DA, Klapper DG & Eddy EM. (1995a) Characterization of Fsc1 cDNA for a mouse sperm fibrous sheath component. *Biol Reprod* 52, 41–49.
Fulcher KD, Welch JE, Klapper DG, O'Brien DA & Eddy EM. (1995b) Identification of a unique mu-class glutathione S-transferase in mouse spermatogenic cells. *Mol Reprod Dev* 42, 415–424.
Hess KC, Jones BH, Marquez B, Chen Y, Ord TS, Kamenetsky M *et al.* (2005) The "soluble" adenylyl cyclase in sperm mediates multiple signaling events required for fertilization. *Dev Cell* 9, 249–259.
Hinsch K-D, De Pinto V, Aires VA, Schneider X, Messina A & Hinsch E. (2004) Voltage-dependent anion-selective channels VDAC2 and VDAC3 are abundant proteins in bovine outer dense fibers, a cytoskeletal component of the sperm flagellum. *J Biol Chem* 279, 15281–15288.
Ihara M, Kinoshita A, Yamada S, Tanaka H, Tanigaki A, Kitano A *et al.* (2005) Cortical organization by the septin cytoskeleton is essential for structural and mechanical integrity of mammalian spermatozoa. *Dev Cell* 8, 343–352.
Ijiri TW, Merdiushev T, Cao W & Gerton GL. (2011) Identification and validation of mouse sperm proteins correlated with epididymal maturation. *Proteomics* 11, 4047–4062.
Johnson LR, Foster JA, Haig-Ladewig L, Vanscoy H, Rubin CS, Moss SB *et al.* (1997) Assembly of AKAP82, a protein kinase A anchor protein, into the fibrous sheath of mouse sperm. *Dev Biol* 192, 340–350.
Korley R, Pouresmaeili F & Oko R. (1997) Analysis of the protein composition of the mouse sperm perinuclear theca and characterization of its major protein constituent. *Biol Reprod* 57, 1426–1432.
Laemmli UK. (1970) Cleavage of structural proteins during the assembly of the head of bacteriophage T4. *Nature* 227, 680–685.
Maiorino M, Roveri A, Benazzi L, Bosello V, Mauri P, Toppo S *et al.* (2005) Functional interaction of phospholipid hydroperoxide glutathione peroxidase with sperm mitochondrion-associated cysteine-rich protein discloses the adjacent cysteine motif as a new substrate of the selenoperoxidase. *J Biol Chem* 280, 38395–38402.
Miki K, Willis WD, Brown PR, Goulding EH, Fulcher KD & Eddy EM. (2002) Targeted disruption of the Akap4 gene causes defects in sperm flagellum and motility. *Dev Biol* 248, 331–342.
Nakamura N, Mori C & Eddy EM. (2010) Molecular complex of three testis-specific isozymes associated with the mouse sperm fibrous sheath: hexokinase 1, phosphofructokinase M, and glutathione S-transferase mu class 5. *Biol Reprod* 82, 504–515.
Oko R & Clermont Y. (1991) Origin and distribution of perforatorial proteins during spermatogenesis of the rat: an immunocytochemical study. *Anat Rec* 230, 489–501.
Oko R & Morales CR. (1994) A novel testicular protein, with sequence similarities to a family of lipid binding proteins, is a major component of the rat sperm perinuclear theca. *Dev Biol* 166, 235–245.
Oko R, Moussakova L & Clermont Y. (1990) Regional differences in composition of the perforatorium and outer periacrosomal layer of the rat spermatozoon as revealed by immunocytochemistry. *Am J Anat* 188, 64–73.
Schneider M, Förster H, Boersma A, Seiler A, Wehnes H, Sinowatz F *et al.* (2009) Mitochondrial glutathione peroxidase 4 disruption causes male infertility. *FASEB J* 23, 3233–3242.
Selvaraj V, Asano A, Page JL, Nelson JL, Kothapalli KSD, Foster JA *et al.* (2010) Mice lacking FABP9/PERF15 develop sperm head abnormalities but are fertile. *Dev Biol* 348, 177–189.
Shalgi R, Seligman J & Kosower NS. (1989) Dynamics of the thiol status of rat spermatozoa during maturation: analysis with the fluorescent labeling agent monobromobimane. *Biol Reprod* 40, 1037–1045.
Sinclair ML, Wang XY, Mattia M, Conti M, Buck J, Wolgemuth DJ *et al.* (2000) Specific expression of soluble adenylyl cyclase in male germ cells. *Mol Reprod Dev* 56, 6–11.
Strader MB, Tabb DL, Hervey WJ, Pan C & Hurst GB. (2006) Efficient and specific trypsin digestion of microgram to nanogram quantities of proteins in organic-aqueous solvent systems. *Anal Chem* 78, 125–134.
Su D, Novoselov SV, Sun Q-A, Moustafa ME, Zhou Y, Oko R *et al.* (2005) Mammalian selenoprotein thioredoxin-glutathione reductase. Roles in disulfide bond formation and sperm maturation. *J Biol Chem* 280, 26491–26498.
Sullivan R, Frenette G & Girouard J. (2007) Epididymosomes are involved in the acquisition of new sperm proteins during epididymal transit. *Asian J Androl* 9, 483–491.
Towbin H, Staehelin T & Gordon J. (1979) Electrophoretic transfer of proteins from polyacrylamide gels to nitrocellulose sheets: procedure and some applications. *Proc Natl Acad Sci USA* 76, 4350–4354.
Triphan X, Menzel VA, Petrunkina AM, Cassará MC, Wemheuer W, Hinsch K-D *et al.* (2008) Localisation and function of voltage-dependent anion channels (VDAC) in bovine spermatozoa. *Pflugers Arch* 455, 677–686.
Visconti PE, Johnson LR, Oyaski M, Fornés M, Moss SB, Gerton GL *et al.* (1997) Regulation, localization, and anchoring of protein kinase A subunits during mouse sperm capacitation. *Dev Biol* 192, 351–363.
Wessel D & Flügge UI. (1984) A method for the quantitative recovery of protein in dilute solution in the presence of detergents and lipids. *Anal Biochem* 138, 141–143.

White DR & Aitken RJ. (1989) Influence of epididymal maturation on cyclic AMP levels in hamster spermatozoa. *Int J Androl* 12, 29–43.
Yeung CH, Sonnenberg-Riethmacher E & Cooper TG. (1999) Infertile spermatozoa of c-ros tyrosine kinase receptor knockout mice show flagellar angulation and maturational defects in cell volume regulatory mechanisms. *Biol Reprod* 61, 1062–1069.

SUPPORTING INFORMATION

Additional Supporting Information may be found in the online version of this article:

Table S1. A detailed statistical analysis of the proteins identified in this study that change their thiol status during epididymal maturation in reduced caput versus non-reduced cauda epididymal sperm cells, non-reduced caput vs. non-reduced cauda epididymal sperm cells, and reduced cauda versus non-reduced cauda epididymal sperm cells. Boxes indicate spots that were identified as two proteins. DIGE analysis was performed. One-way analysis of variance (ANOVA) *p*-values, Student's *t*-test *p*-values, and average volume ratios were calculated with DeCyder software v5.01 by using the mixed-sample internal standard methodology. ND, not determined. *See text for discussion.